out separately, by means of an axially and radially movable probe. We found, by interferometry, that the wave signals were primarily concentrated within the axial length of the T probes or grids. When the detecting probe was outside of this region, the signal dropped by 60 dB. Our measurements indicated that in the axial direction the waves were essentially standing waves, with the dominant Fourier components having twice the probe lengths; i.e., $k_{\parallel}' \simeq \pi/l'$, etc. Thus, by approximating the standing waves in the axial direction with $\cos(k_{\parallel}'z)$, $\cos(k_{\parallel}''z)$, we find from theory that for $k_{\parallel} \ll k_{\perp}$ the dominant contributions to the matrix elements are given by $k_{\parallel} = k_{\parallel}' + k_{\parallel}''$. By varying the lengths of the receiving and transmitting probes in the nonlinear Landau damping experiments, we have verified that this model of wave excitation gave good agreement with theory.

In summary, we believe that we have observed experimentally nonlinear Landau damping of plasma waves in the presence of an external magnetic field. The qualitative features of the experimental results agreed well with the predictions of the nonlinear Landau damping theory. In particular, the observed decay of a finite-amplitude wave into a single perturbed wave cannot be explained by resonant mode-mode coupling or parametric theory. The amplitude variation of the perturbed wave as a function of the pump wave followed the predictions of the third-order theory, through at least four decades. The measured nonlinear wave-particle coupling coefficient was found to agree with theory within experimental error. A detailed account of this work will be published elsewhere.

We are very grateful to Professor M. N. Rosenbluth and Professor B. Coppi for invaluable discussions. Technical assistance received from J. Semler, K. Mann, and W. Lamont is acknowledged. We thank H. Fishman for performing the numerical integrations.

*Work performed under the auspices of the U. S. Atomic Energy Commission, Contract No. AT(30-1)-1238.

[1]R. Z. Sagdeev and A. A. Galeev, in *Nonlinear Plasma Theory,* edited by T. M. O'Neil and D. L. Book (Benjamin, New York, 1969), p. 89.

[2]R. E. Aamodt and W. E. Drummond, Phys. Fluids 7, 1816 (1964), and in *Proceedings of a Conference on Plasma Physics and Controlled Nuclear Fusion Research, Culham, England, 1965* (International Atomic Energy Agency, Vienna, Austria, 1966), Vol. I, p. 435.

[3]M. N. Rosenbluth, B. Coppi, and R. N. Sudan, Ann. Phys. (New York) 55, 207 (1969).

[4]I. B. Bernstein, Phys. Rev. 109, 10 (1958).

[5]M. Porkolab and R. P. H. Chang, Phys. Rev. Lett. 22, 826 (1969).

[6]R. P. H. Chang and M. Porkolab, to be published.

[7]In the spatial case, the finite parallel wave number cannot be neglected in nonlinear Landau damping theory in a nearly collisionless plasma.

[8]The dispersion curves shown in Fig. 1(b) are those with $k_{\parallel}=0$. Nevertheless, for the experimentally measured values of $k_{\parallel}/k_{\perp}(k_{\parallel} \ll k_{\perp})$, it can be shown that the *real* parts of $k_{\perp}$ and ω are closely approximated by the curves used.

[9]M. Porkolab and J. Sinnis, Phys. Rev. Lett. 21, 1227 (1968).

Electron Cyclotron Drift Instability*

D. W. Forslund, R. L. Morse, and C. W. Nielson
Los Alamos Scientific Laboratory, University of California, Los Alamos, New Mexico 87544
(Received 30 July 1970)

Electron cyclotron waves are shown to grow unstably in the presence of small relative drifts of a warm ion distribution perpendicular to the B field. Numerical simulations show that this instability causes anomalous diffusion of plasma across the magnetic field and heating of the electron thermal spread to values much greater than the relative ion-electron drift velocity.

Most methods for heating and confining high-temperature plasma involve a flow of electric currents normal to magnetic field lines in the plasma. This Letter reports the theoretical properties of a high-frequency electrostatic plasma instability which is driven by the relative drift of ions and electrons in such a normal current flow and which is expected to occur and cause anomalous resistance to the current in a wide range of applications. The calculations presented here are done for an infinite, uniform, collisionless plasma with a fixed magnetic field B_z. The electrons have no drift and the ions have a drift v_d in the x direction. The ion and electron temperatures are $T_i = Mv_i^2/2$ and $T_e = mv_e^2/2$.

Because the growth rates are large compared with the ion cyclotron frequency, the ions are assumed to have straight-line trajectories; and the appropriate dispersion relation for normal linearized electrostatic waves of the form $E_x \sim \exp[i(kx-\omega t)]$ is the dispersion relation of Bernstein[1] for electron cyclotron waves with an additional term, the Z' function,[2] added to give the ion contribution to the perturbed charge density:

$$(K\lambda_D)^2 = -1 + e^{-\lambda} I_0(\lambda) + 2\omega^2 \sum_{n=1}^{\infty} \frac{e^{-\lambda} I_n(\lambda)}{\omega^2 - (n\Omega_e)^2} + \frac{T_e}{2T_i} Z'\left(\frac{\omega - kv_d}{kv_i}\right). \tag{1}$$

Here $\Omega_e = eB_z/mc$ is the electron cyclotron frequency, $\lambda + (kr_e)^2/2$, $r_e = v_e/\Omega_e$ is the mean electron gyroradius, and λ_D is the Debye length. Figure 1(a) illustrates the source of the instability. Values of ω/Ω_e for the first three harmonics of the electron cyclotron waves are plotted against kr_e together with straight lines of slope $\omega/k = v_d$ and $v_d \pm v_i$ for the case $\omega_p/\Omega_e = 1.0$, $v_d = 0.75 v_e$, $T_e = T_i$, and $m/M = 1/100$. The instability results from a resonance between the otherwise purely real electron cyclotron waves and ions on the positive-slope side of the ion distribution ($v_d > 0$), i.e., with velocities less than v_d. Modes with some $\bar{k}$ parallel to B_z will grow more slowly because of Landau damping of the electron cyclotron waves. Because the instability is resonant with the ions, the maximum growth rate for each harmonic occurs near the point of maximum slope of the ion velocity distribution, which is about where the electron-wave curves intersect the dashed line $\omega/k = v_d - v_i$. In fact, all electron cyclotron waves to the right of the line $\omega/k = v_d$ are unstable with the reservation that the growth rates and initial fluctuations must be large enough that nonlinear distortion of velocity distributions occurs in less than an ion gyro period.

This instability would not, however, be seen experimentally as electron cyclotron noise in the ion frame, which is usually the lab frame, because of the drift-velocity Doppler shift. In the limit of small v_d/v_e where growth rates are smaller and the resonances occur at large kr_e, the electron wave frequencies are asymptotic to the cyclotron harmonics. Substituting $\omega = \omega_R + i\gamma$ into Eq. (1) and assuming $|\gamma| \ll |\omega_R|$ gives an estimate of the growth rate of the nth harmonic:

$$\frac{\gamma}{\Omega_e} \simeq \frac{n}{2\pi^{1/2} kr_e} \frac{T_e}{T_i} \frac{\mathrm{Im} Z'((\omega_R - kv_d)/kv_i)}{[1 + (k\lambda_D)^2 - (T_e/2T_i)\,\mathrm{Re} Z'((\omega_R - kv_d)/kv_i)]^2}. \tag{2}$$

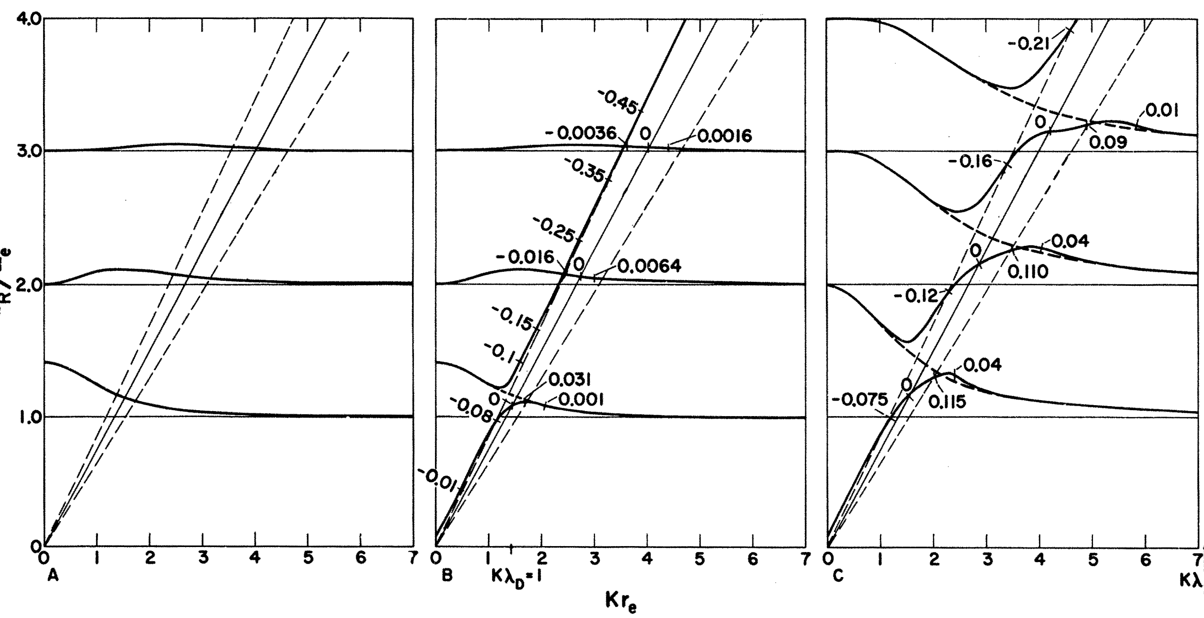

FIG. 1. (a) The superposition of ω_R/Ω_e vs Kr_e for the first three electron cyclotron harmonics and diagonal straight lines at the velocities $v_d + v_i$ (upper dashed line), v_d (solid line), and $v_d - v_i$ (lower dashed line), for the case $\omega_p/\Omega_e = 1.0$, $T_e/T_i = 1.0$, $m/M = 1/100$, and $v_d/v_e = 0.75$. (b) The same as (a) but with the exact solutions of the dispersion relation including indicated values of the growth rate γ/Ω_e. (c) The exact solution for the case $\omega_p/\Omega_e = 5$, $T_e/T_i = 1.0$, $m/M = 1/100$, and $v_d/v_e = 0.75$.

For all $\omega_R < kv_d$, γ/Ω_e is positive corresponding to unstable growth. From this expression one can see that (1) when $k\lambda_D > 1$ there is a $(k\lambda_D)^{-4}$ attenuation of growth rates, which produces an effective cutoff for large $k\lambda_D$; (2) for kr_e large but $k\lambda_D < 1$ all harmonics have about the same growth rate because the resonance condition is $kr_e \simeq nv_e/(v_d - v_i)$; (3) because of this condition and the fact that the maximum of ImZ' is about 1, γ is of the order of $\Omega_e v_d/v_e$ when $v_d > v_i$ and $k\lambda_D < 1$; (4) the growth rates are essentially independent of the electron-ion mass ratio; (5) the Debye length cutoff occurs at smaller values of v_d/v_e in cases of larger ω_p/Ω_e because of the form of the resonance condition above and the fact that $k\lambda_D = kr_e(\Omega_e/\sqrt{2}\omega_p)$. Therefore more harmonics will grow in cases with larger ω_p/Ω_e.

Figures 1(b) and 1(c) are plots of ω_R/Ω_e vs kr_e with indicated values of γ/Ω_e from computed solutions of Eq. (1) for the case illustrated in Fig. 1(a) and for the case $\omega_p/\Omega_e = 5.0$, $v_d = 0.75v_e$, $T_e = T_i$, and $m/M = 1/100$. For $(k\lambda_D)^2 \lesssim 1$ there is a strong interaction between the electron cyclotron mode and the ion mode as implied by the presence of the ReZ' term in the denominator of Eq. (2). This distortion results in the topological connection of the harmonic number n with $n+1$, where the $n=0$, $k=0$ undamped mode is just the lower hybrid frequency.

It should be noted that the effect of temperature ratio and mass ratio is relatively weak for this instability. For the set of parameters shown in Fig. 1(c) but with $0 < T_i/T_e < 5$, the maximum growth rate ranges over $0.16\Omega_e > \gamma_{\max} < 0.04\Omega_e$. For the mass ratio $M/m = 1836$ and the same range of temperature, the maximum growth-rate range is $0.064\Omega_e > \gamma_{\max} > 0.04\Omega_e$. Although the instability is nonresonant with the ions for $T_e \gg T_i$, the growth rates are only slightly increased over those in the resonant region.

The Debye length cutoff implies, of course, that the instability is most effective with $\omega_p \sim \Omega_e$ for drifts large compared with the electron thermal speed. With the assumptions of phase velocity greater than the electron or ion thermal speed, Eq. (1) reduces to[3]

$$1 = \frac{1}{\omega^2/\omega_p^2 - \Omega_e^2/\omega_p^2} + \frac{m/M}{(\omega/\omega_p - kv_d/\omega_p)^2}.$$

For $\Omega_e/\omega_p \ll 1$ this equation gives the usual two-stream instability. Physically, this equation can be thought of as the interaction of the upper hybrid mode with the Doppler-shifted lower hybrid mode. A necessary condition for instability is $kv_d > \Omega_e$. For $\Omega_e/\omega_p \sim 1$ the mode is quite different from the two-stream instability but has a maximum growth rate only slightly less than the maximum two-stream value.

Thus the range of parameters which give rise to rapidly growing waves is not limited to $T_e \gg T_i$ and $\omega_p \gg \Omega_e$ as implied by Wong[4] who also considered the dispersion relation of Eq. (1). As a consequence there is instability when ion acoustic waves in the absence of a magnetic field would otherwise be stable.

There appear to be three conditions under which this instability would be squelched: (1) when the current drift is removed, which could result from field diffusion caused by the instability; (2) when the instability heats the electrons to the Debye-length cutoff; (3) when the ions are resonantly heated until the maximum of ImZ' for the fundamental is very small and/or lies beyond the Debye-length cutoff. When $v_d \ll v_e$ and $\omega_p/\Omega_e \gg 1$, sufficient electron heating is more difficult to achieve and the third condition, ion heating, is more important. This instability, unlike the ion-acoustic instability,[5] can be an effective ion-heating mechanism because the resonance occurs at or near the point of maximum slope of the ion velocity distribution.

Numerical simulations of the nonlinear development of this instability have been done by the particle-in-cell method[6] in the three-dimensional phase space (x, v_x, v_y) with a fixed B_z and an artificial gravity, g_y, applied to the electrons to give the drift v_d. The effect of the B_z field on the ion motion is included in the simulations. Figure 2(a) is the total E_x field energy as a function of time in plasma periods for a run corresponding to Fig. 1(b). Figure 2(b) is the energy history for the first 200 of a total of 400 plasma periods of a run corresponding to Fig. 1(c). In both cases the computed and simulation growth rates agree to within a few percent as they do for a number of other runs that have been made. Wavelengths of maximum growth rate also agree within the limits of grid-length quantization. Full scale on Fig. 2(a) is 0.16 times the total initial electron thermal energy and on Fig. 2(b) full scale is 0.05. The long-time-scale oscillations in Fig. 2(b) indicate repeated development, saturation, and decay of the resonant instability at the wavelength predicted by the linear theory. The instability forms repeatedly near the point of maximum slope of the ion velocity distribution, which point changes in time because of resonant heating of ions and because of ion gyro mo-

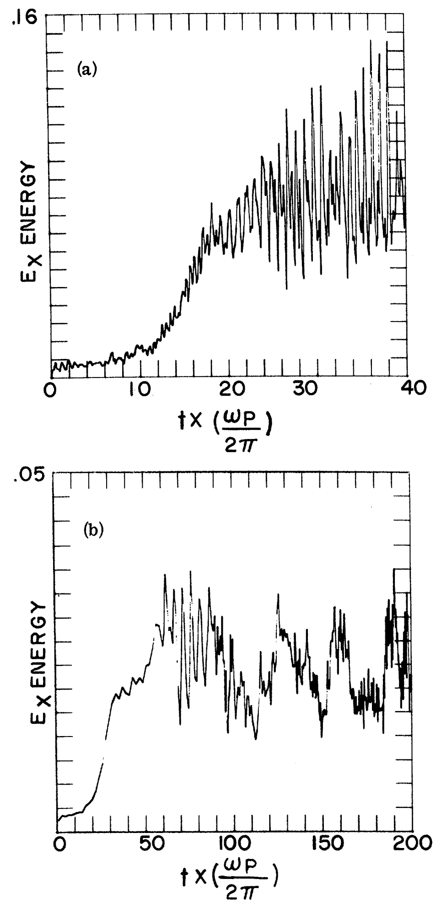

FIG. 2. Electrostatic field-energy histories from the two cases treated here. The full-scale energies are in units of the total initial electron thermal energy.

tion. The 400 plasma periods constitute 0.8 ion gyro period in this second case. During this time the ion thermal spread, v_i, increases by a factor of 1.7, or a temperature increase of 3.0; and the electron thermal spread, v_e, increases by 3.6 to a remarkably large 4.8 times v_d. The electrons of course remain quite isotropic in velocity because of gyro motion.

In addition to heating the plasma, the effective electrical resistance of the turbulence produces a drift and diffusion across the B_z field in the y direction. In the simulation computations the motion of the guiding-center position, y_g, of each simulation particle is followed by integrating the equation for canonical momentum (written here for electrons),

$$dP_x/dt=-eE_x, \tag{3}$$

and using the fact that in a uniform B_z field the definition gives

$$P_x=mv_x-eA_x/c=mv_x+eB_zy/c=m\Omega_e y_g \tag{4}$$

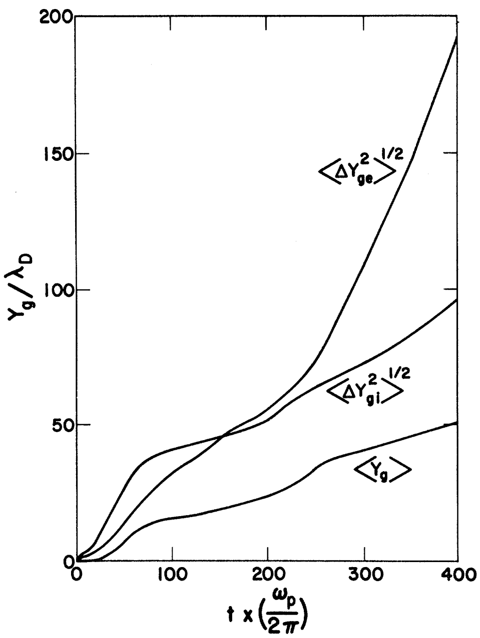

FIG. 3. Mean guiding-center displacement $\langle y_g\rangle$ and root mean square spread of electron guiding centers $\langle\Delta y_{ge}{}^2\rangle^{1/2}$ and ion guiding centers $\langle\Delta y_{gi}\rangle^{1/2}$ about this mean, from the simulation of the second case [Fig. 2(a)]. These results clearly show anomalous diffusion perpendicular to the magnetic field.

because the particle's y position for $v_x=0$ is that of its guiding center. Figure 3 shows the time dependence of the mean guiding-center position, $\langle y_g\rangle$, in the case $\omega_p/\Omega_e=5$ [Figs. 1(c) and 2(b)] for both particle species—they must be equal because of momentum conservation—and the root mean square deviations about this mean, $\langle\Delta y_{ge}{}^2\rangle^{1/2}$ and $\langle\Delta y_{gi}{}^2\rangle^{1/2}$, in units of the initial Debye length, which can be converted to units of c/ω_p if β of the plasma is given. Such a resistive slippage of plasma across magnetic field is often associated with subcritical collisionless shock waves.[7] More generally, because lower values of v_d/v_e are required by the Debye length cutoff in cases of larger ω_p/Ω_e, regions of low magnetic field in many shock and pinch device plasmas, including regions of field reversal, should be susceptible to this instability. However, in some experimental situations the instability demonstrated here may be prevented from developing by Coulomb collisions of the electrons at a frequency of the order of the growth rate, i.e., approaching the electron cyclotron frequency Ω_e. Thus plasma resistivity might be larger for conditions giving very low and very high collision frequencies with a minimum in between.

Linear analysis including a time-varying magnetic field indicates that this instability is essentially longitudinal until particle energies become relativistic. One- and two-dimensional numerical simulation of the cases treated here by a fully electromagnetic simulation method[8] and with an initial electron temperature of 17 keV ($V_{the}/c=0.25$), i.e., an electron $\beta_e=(5/4)^2$ when $\omega_p/\Omega_e=5$, have shown the development of the instability to be essentially unchanged by finite β_e effects.

The reader may be interested to know that the instability presented here was initially found with the numerical simulation code.

The authors are grateful to Dr. E. Hintz for encouraging study of anomalous resistivity in connection with low Mach-number collisionless shocks.

*Work performed under the auspices of the U. S. Atomic Energy Commission.

[1] I. B. Bernstein, Phys. Rev. 109, 10 (1958).
[2] B. D. Fried and S. D. Conte, *The Plasma Dispersion Function* (Academic, New York, 1961).
[3] O. Buneman, J. Nucl. Energy, Part C 4, 111 (1962).
[4] H. V. Wong, Phys. Fluids 13, 757 (1970).
[5] R. L. Morse and C. W. Nielson, "Turbulent Heating of Hydrogen" (to be published).
[6] R. L. Morse and C. W. Nielson, Phys. Fluids 12, 2418 (1969) and Phys. Rev. Lett. 23, 1087 (1969); R. L. Morse, in *Methods in Computational Physics*, edited by B. Alder, S. Fernbach, and M. Rotenberg (Academic, New York, 1970), Vol. 9, p. 213.
[7] A. G. Es'kov, R. Kh. Kurtmullaev, A. I. Malyutin, V. I. Pil'skii, and V. N. Semenov, Zh. Eksp. Teor. Fiz. 56, 1480 (1969) [Sov. Phys. JETP 29, 793 (1969)].
[8] R. L. Morse and C. W. Nielson, "Numerical Simulation of the Weibel Instability in One and Two Dimensions" (to be published).

Magnetic Field Splitting of the Quasiparticle States in Superconducting Aluminum Films

R. Meservey and P. M. Tedrow
Francis Bitter National Magnet Laboratory, Massachusetts Institute of Technology, Cambridge, Massachusetts 02139*

and

Peter Fulde
Institut für Theoretische Physik der Universität Frankfurt am Main, Frankfurt am Main, Germany
(Received 4 September 1970)

Magnetic field splitting of the quasiparticle energy states in superconducting aluminum films has been observed in a tunneling experiment. The magnitude of the splitting was found to be $2\mu H$, and is attributed to the magnetic moment of the quasiparticles. The observed tunneling conductance is in qualitative agreement with theory.

We have observed splitting of the quasiparticle states in thin superconducting aluminum films in a parallel magnetic field. The density of states was obtained[1,2] by measuring the tunneling conductance, dI/dV, of Al-Al_2O_3-Ag junctions as a function of voltage V for various applied magnetic fields, H.

In the absence of a magnetic field the quasiparticle energy spectrum in a superconductor is given by the Bardeen, Cooper, and Schrieffer (BCS) theory[3] to be $E=(\epsilon^2+\Delta^2)^{1/2}$, where ϵ is the kinetic energy measured from the Fermi surface and 2Δ is the energy gap. A magnetic field applied to a thin superconducting film will act on the spins of the electrons as well as on their orbits. Both interactions will change the quasiparticle spectrum. If the film is thin enough, however, the effect of the field on the electron orbits will be negligible compared with the effect on the electron spins, provided the spin-orbit scattering rate is sufficiently small. In this case the quasiparticle spectrum becomes simply $E_{\uparrow,\downarrow}=(\epsilon^2+\Delta^2)^{1/2}\pm\mu H$, where μ is the electron magnetic moment. It will be shown later that our samples fulfill the above conditions. As a consequence we would expect the total tunneling density of states to consist of the addition of two BCS-type density-of-states curves shifted in voltage by $\pm\mu H/e$ with respect to the curve in the absence of field.[4]

This behavior has been observed experimentally as shown in Fig. 1, where $(dI/dV)_s$ is plotted versus V for various values of H. The magnitude of $(dI/dV)_s$ has been normalized to the normal-state conductance, $(dI/dV)_n$. According to theory we expect that the energy change of the peaks in the spin-up and spin-down density of states should be proportional to $\pm H$. Figure 2 shows a plot of the positions of these peaks as a function of H. The spin splitting agrees well with the simple theory given above over the entire range of field.